Impact on the Wave Parameters Estimation of a Kinetic Energy Harvester Embedded into a Drifter

Matias Carandell
SARTI Group,
Electronic Engineering Department
Universitat Politècnica de Catalunya
Vilanova i la Geltrú, Spain
matias.carandell@upc.edu

Daniel Mihai Toma
SARTI Group,
Electronic Engineering Department
Universitat Politècnica de Catalunya
Vilanova i la Geltrú, Spain
daniel.mihai.toma@upc.edu

J.P. Pinto
Divisão de Oceanografia
Instituto Hidrográfico
Lisbon, Portugal
paulo.pinto@hidrografico.pt

Manel Gasulla
e-CAT Group,
Electronic Engineering Department
Universitat Politècnica de Catalunya
Castelldefels, Spain
manel.gasulla@upc.edu

Joaquín del Río
SARTI Group,
Electronic Engineering Department
Universitat Politècnica de Catalunya
Vilanova i la Geltrú, Spain
joaquin.del.rio@upc.edu

Abstract— The effect of a Kinetic Energy Harvester (KEH) on the wave parameters estimation at a WAVY Ocean (WO) drifter is being studied. An algorithm has been developed to calculate the wave parameters from the Inertial Measuring Unit (IMU) embedded on the drifter. Simulations performed by OrcaFlex have been used to refine the algorithm and assess the measurement errors derived from the drifter response. Finally, a WO prototype has been deployed in the controlled environment of CIEM wave flume. Results prove that the KEH has no significant impact on the wave parameter estimation.

Keywords*— Lagrangian Drifter, Kinetic Energy Harvester (KEH), Inertial Measurement Units (IMU), Significant Wave Height, Significant Wave Period, Natural Frequency and Resonance.*

I. Introduction

Lagrangian drifters are autonomous floating passive devices that provide oceanographic surface data. They are low-cost, versatile and easy-deployable marine instrumentation used in climate research, oil spill tracking, or search and rescue operations. The EC-funded MELOA project [1] aims to develop a new family of spherical drifters (WAVY) for marine monitoring. The WAVY family of products will include from coastal drifters for short deployments, to oceanic drifters with energy scavenging solutions for long term deployments. One of these units under design is the WAVY Ocean (WO) drifter, whose aim is to generate sea data as the wave intrinsic parameters (height, period and direction) and send it through a satellite link. Acquiring these in-situ measurements provides valuable data which can be used to calibrate satellite ocean observation systems [2] or wave forecast models. As shown at [3], GPS data has lately been used to calculate these wave intrinsic parameters. The common methodology is to use the differential GPS position to estimate the vertical velocity of the unit and then obtain its displacement. From the displacement spectrum of the wave its intrinsic parameters can be obtained [4]. Nowadays, modern Inertial Measuring Units (IMU) allow to measure drifter's motion at higher frequencies with low-cost solutions, so the ocean surface interaction with the air can be studied [5], not only the slow wave components.

One of the main challenges related to the drifter's design is the autonomy [6]. Some companies offer drifters with PV solar panels that at some sampling interval may work at "perpetual" lifespan. (Sofar: Spotter, Fastwave: Voyager Solar). Nevertheless, drifters strictly dedicated to monitor superficial ocean currents should not be exposed to wind because it may affect the current tracking [7]. Consequently, they must be mostly submerged and the sunlight at PV panels may be greatly attenuated by the water. For this reason, we started to explore other Energy Harvester (EH) sources as the kinetic oscillatory movement of the waves. This is usually done by inertial systems. These systems rely on a proof mass which moves in relation to the main body thanks to the excitation of the waves. However, having a moving mass inside the drifter may cause interferences in the IMU sensor and so in the wave parameter estimation.

As studied in [8], in some sea conditions the drifter may not strictly follow the slope of the sea-surface affecting also in the wave parameters estimation. That happens when the drifter response enters in resonance with the sea waves excitation. This resonance may occur when the natural frequency of the drifter matches with the fundamental frequency of the waves or, according to [9], with one of the non-linear induced harmonics in the drifter movement. Resonance effects may be beneficial for the energy production of an inertial system. Thus, some works demonstrated how tuning the buoy parameters to enhance the resonance maximize the power extraction of a Wave Energy Converter (WEC) [10]. Nevertheless, if the drifter aims to estimate the wave parameters it should follow the slope of the sea-surface and resonance effects may worsen these measurements.

The objective of this work is to study the effect of an inertial system such as a kinetic EH (KEH) on the wave parameter estimation at the WO. To evaluate this possible impact, a MATLAB algorithm has been designed to calculate the wave parameters from the embedded IMU. A simulation tool has then been used to refine this algorithm and estimate its error in critical situations as resonance drifter events. Then, a WO prototype as the one presented in [11] has been deployed in a controlled environment with and without its

This work was supported by the project MELOA from the European Commission's Horizon 2020 research and Innovation program under Grant Agreement No. 776280. The first author has a grant from the Secretariat of Universities and Research of the Ministry of Business and Knowledge of the Government of Catalonia on the FI program (ref. BDNS 362582).

KEH system and results has been analyzed to determine its effect.

The paper is organized as follows. First, the wave parameters estimation method is described in Section II. Section III describes the materials and method used to obtain the simulation and experimental data, which are summarized and discussed later in section IV. Finally, Section 0 concludes the work.

II. Estimation of the Wave Parameters

Sea surface is composed of different types of waves; thus, it is normally characterized by statistical parameters. Wave parameters can be estimated by evaluating the time series of the sea elevation (D_z) from a single point. The zero-crossing method uses the Still Water Level (SWL) reference from the time series data to characterize each single wave by its period and height (Fig. 1). By ranking them, multiple common parameters can be obtained. The significant wave height (H_3) is the mean height of the third highest waves in the record and the significant wave period (T_3) is the corresponding mean period. The maximum wave height (H_{max}) is simply the largest measured wave in the record and its period is known as maximum wave period (T_{max}).

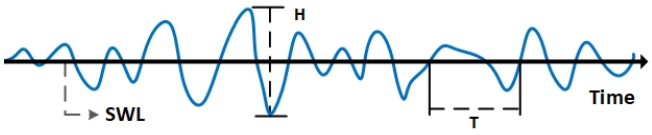

Fig. 1. Time series of the sea surface displacement, where the Still Water Level (SWL) is used on the zero-crossing method to obtain Height (H) and Period (T).

A different approach can be given with the spectral analysis. This study provides the equivalent wave parameters by using the Fast Fourier Transform (FFT) of the sea elevation. The resulting power spectral density shows how the energy density is distributed among frequencies and its power momentums are related with the wave parameters. To provide a complete analysis of a real sea state both approaches (zero-crossing and spectral) must be considered. Nevertheless, in this study we will work in a controlled experimental environment that generates monochromatic waves, with a single height and period. In this case, only the zero-crossing method will be considered.

To obtain the sea elevation (D_z) from the IMU on a floating device and, thus, the wave parameters, the acceleration (a_x, a_y, a_z) and gyroscope (g_x, g_y, g_z) data are normally used [12]. Specifically, in this work, to smooth out accelerometer's errors due to vibration and mechanical noise, a weight linear combination technique of both has been considered to estimate new IMU accelerations. A high-pass Lanczos filter [13] has then been used in the time domain of a_z to remove the slow motion and the gravity acceleration offset, resulting in the wave orbital acceleration (a_{woz}). Then, the vertical velocity has been obtained performing a time integration by blocks of 20 waves, forcing zero average for each integrated block as an additional condition to deal with the unknown integration constant.

$$v_z = \int a_{woz}(t)dt \tag{1}$$

Again, the high-pass Lanczos filter has been used on v_z to remove low frequency components generated by the integration scheme. Finally, the vertical displacement has been obtained by integrating the velocity in the time domain.

$$D_z = \int v_z(t)dt \tag{2}$$

Both integration steps work also as a low-pass filter because they remove the high frequency components as the natural frequency of the drifter (f_n), which is the response of the drifter when placed on a fluid. This can be obtained from

$$\omega_n{}^2 = \frac{\frac{\partial F_B}{dz}\Big|_{z=d}}{m_b+m_f} \tag{3}$$

where ω_n is the angular natural frequency, m_b is the total drifter mass and m_f is the drifter hydrodynamic mass. F_B is the buoyancy force and d is the distance between the SWL and the geometric center (c_g). m_f can be estimated as

$$m_f = \rho V_{sub} C_a \tag{4}$$

where ρ is the fluid density, C_a is the added mass coefficient (0.5 for a sphere) and V_{sub} the submerged volume in still water conditions. V_{sub} is obtained as

$$V_{sub} = \frac{\pi}{3}(2R^3 + 3\,R^2 d - d^3) \tag{5}$$

where R is the radius of the buoy. Also, F_B is given by

$$F_B = \rho g V_{sub} \tag{6}$$

where g is the gravity acceleration. Using (3) – (6), ω_n results

$$\omega_n{}^2 = \frac{\rho g \pi (R^2 - d^2)}{m_b + \frac{\rho\pi}{6}(2R^3 + 3R^2 d - d^3)} \tag{7}$$

Finally, the natural frequency of the vertical movement of a spherical drifter when an external excitation sinks it can be obtained from

$$\omega_n = 2\pi f_n \tag{8}$$

Z. Ballard obtained at [14] a similar approach to obtain f_n, with some minor changes due to a different approach on the system vertical reference.

III. Materials and Method

To evaluate the possible impact of a KEH in the wave parameters estimation by the WO drifter and following the Section II procedure, a MATLAB algorithm has been designed to calculate H_3 and T_3 from the linear and angular accelerations. This algorithm can be used both with the experimental data provided by an IMU embedded in a WO and with the data provided by a simulated drifter. It can also be used if the vertical displacement is provided, with no filter and time integration steps applied, just using the zero-crossing method.

First, OrcaFlex software (Orcina) has been used to refine the algorithm and estimate its error in critical situations as resonance drifter events. Then, an WO prototype as the one presented in [11] has been deployed in a controlled environment with and without a KEH system and results have been analyzed to determine its effect. Four MELOA WAVY Littoral (WL) drifters have also been used around the WO to estimate the dispersion of the error on the experimental conditions.

A. Simulation setup

OrcaFlex (Orcina), a dynamic analysis software for offshore marine systems, has been used. The WO prototype has been modeled with a sphere composed by 24 stacked flat cylinders of appropriate diameters and the parameters exposed on TABLE I. The embedded KEH has not been modeled due

to software limitations, so the simulation phase has only been used to evaluate the accuracy of the wave estimation algorithm and tune its internal parameters.

TABLE I. Simulation parameters used in Orcaflex

Symbol	Parameter	Value	Units
m_b	Drifter mass	3.7	kg
R	Drifter radius	0.1	m
ρ	Fluid density	1000	kg/m^3
C_a	Added mass coeff.	0.5	-
d	SWL to c_g distance	0.05	m
$\hat{z}$	c_g to c_m distance	0.04	m

The sea waves were modelled using the Airy model [15], which gives an essential sea state pattern by assuming a sinusoidal surface movement. This model was selected because it matches with the waves generated later in the experimental controlled environment. Four sea conditions were simulated and are listed on TABLE II. The accelerations and angular velocities generated by OrcaFlex, obtained in the mass center (c_m) of the oceanic drifter, were used by the MATLAB algorithm to calculate the D_z and, thus, the wave parameters (H_3 and T_3) through the zero-crossing method. Then, the obtained results have been compared with the actual simulated wave parameters to validate the algorithm. For the simulation procedure, the Lanczos filter cutoff frequency (f_{co}) has been 0.02 Hz.

TABLE II. Simulated sea conditions on OrcaFlex.

Test	H (m)	T (s)	Duration (min)	Sea model
1	0.2	2	5	Airy
2	0.2	3	5	Airy
3	0.3	2	5	Airy
4	0.3	3	5	Airy

Furthermore, an exhaustive analysis has been made in the resonance events, where the matching of f_n with some of the wave spectra components can alter the vertical movement and, thus, induce errors on the wave parameter estimation. For this purpose, H_3 has been obtained using the algorithm with different parameters resulting from the simulation; sea vertical displacement, sea vertical acceleration, drifter vertical displacement and drifter vertical acceleration. Using these data, the different steps of the algorithm can be validated while the resonance effect is assessed.

B. *Experimental setup*

The experimental test was performed on the controlled environment of the Maritime Research and Experimentation Wave Flume (CIEM). The flume is a 100 m long, 3 m wide, and up to 7 m deep channel capable of reproducing waves with heights up to 1.6 m. The system is hydraulically actuated and PC-controlled allowing it to generate known sea states. Resistive sensors extended among the flume provide the real water's surface elevation at 40 Samples Per Second (SPS) with an uncertainty of ±1 cm. Tests from TABLE II were done and tests 3 and 4 were performed twice to assess the effect of the moving mass on the wave estimation with and without the KEH. For the experimental process, f_{co} has been 0.125 Hz.

To fulfill this work's objective, a WO prototype presented in a previous work [11] and shown in Fig. 2 has been used. It counts on a novel KEH system which uses the motion of the waves to generate power. The KEH consists of an articulated pendulum arm with a prof mass. This mass relatively moves with respect to the drifter with pendulum motion. Then, through a gear system, rotation is accumulated in a flying wheel which drives a DC electrical generator. The WO prototype was designed to embed the KEH and perform real sea tests in which to measure its motion and analyze how it traduces into energy production. Therefore, it counts on a three-axis accelerometer and gyroscope IMU (MPU-9250, Invensense) acquiring at 50 SPS and a measurement system which provides the generated power on the KEH. Results of a first test at sea presented at [11], with significant wave height of 1.43 m and significant wave period of 3.45 s, show a net mean power of the 179 µW with peaks of 2.2 mW.

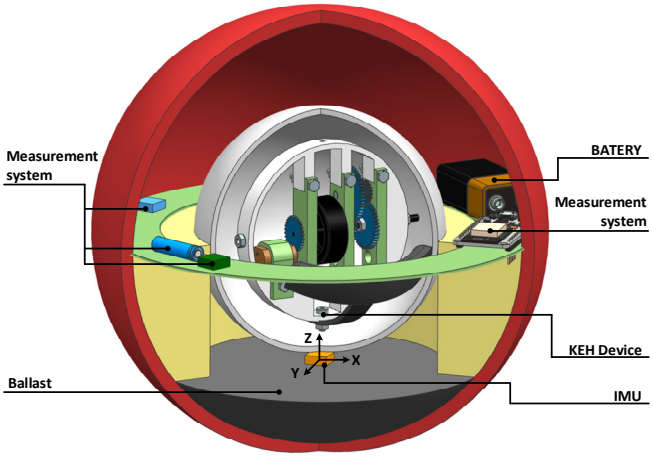

Fig. 2. 3D model of the oceanic drifter prototype with the KEH embedded, the IMU sensor and electronics for measurement.

Also, four WL drifters [1] have been nointly used with the WO prototype. These are smaller units (R = 0.12 m and m_b = 0.76 kg) without harvesting devices, equipped with an IMU (ICM-20690, Invensense) and a sampling rate of 4-6 SPS. The aim of using these littoral drifters is to obtain the standard deviation of the error of H_3 and T_3 parameters for each test. The results obtained with the WO prototype, with and without the KEH, have been compared with the standard deviation of the error to evaluate the possible effect of the moving mass. Fig. 3 shows both drifter units before the experimental test.

Fig. 3. At left, four WAVY Littoral drifters developed by MELOA consortium, at right, the ocean drifter prototype.

IV. Results

A. *Simulation results*

This section shows the results of the simulation phase. OrcaFlex resulting accelerations (a_x, a_y, a_z) and angular velocities (g_x, g_y, g_z) have been used to obtain the sea vertical displacement (D_z) and then H_3 and T_3 through the zero-crossing method. As a first step, the algorithm has been validated. Fig. 4 shows the Power Spectral Density (PSD)

evolution among the D_z obtention process at simulated conditions of Test 3. As can be seen in Fig. 4A, the PSD of a_z contains the gravity acceleration offset which is filtered at a_{woz} after the weight linear combination technique and the first Lanczos filter. Besides the fundamental harmonic placed at f_0 = 0.33 Hz (3 s), Fig. 4B shows that a_{woz} has higher frequency components at the second harmonic ($2 \cdot f_0$ = 0.66 Hz) and the third harmonic ($3 \cdot f_0$ = 1.0 Hz), which agrees with the non-linear wave theory [9]. On the other hand, and according to equation (7) presented at Section II, using the oceanic drifter prototype parameters of TABLE I, a natural frequency of f_n = 0.98 Hz driven by vertical disturbances in buoyancy equilibrium is predicted. This value does not depend on the wave forcing period and it was confirmed in the different simulated tests. So, f_n adds up with the third harmonic so it is a singular case of resonance between the WO and the sea excitation. The wave orbital velocity (v_z) is shown at Fig. 4C, which after the first integration and the second Lanczos filter has removed its high-frequency components. Finally, at Fig. 4D the PSD of D_z is shown with just the wave elevation fundamental harmonic frequenc.

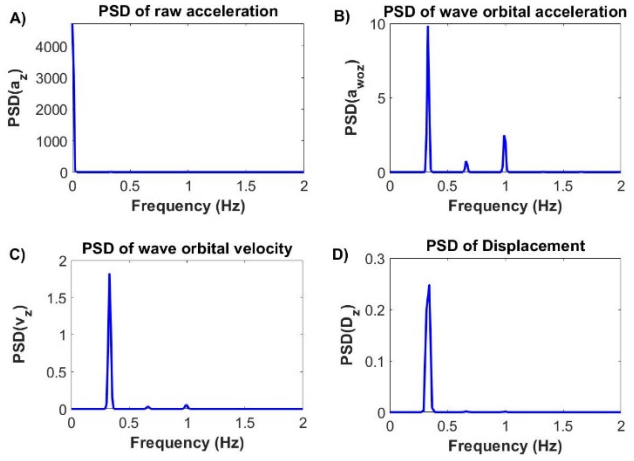

Fig. 4. Power Spectral Density (PSD) evolution among the Displacement obtention process at simulated Test 3 conditions. At A, PSD of vertical acceleration, at B, PSD of wave orbital vertical acceleration, at C, PSD of wave orbital vertical velocity and at D, PSD of vertical displacement.

After obtaining the sea displacement (D_z), the significant wave height and period have been calculated for all the simulated sea conditions of TABLE II with the zero-crossing method. TABLE III shows the results with the absolute error for both parameters. The mean error among the four tests of H_3 is 2 mm with a Root-Mean-Square Deviation (RMSD) of 5 mm. The mean error of T_3 is 13 ms with a RMSD of 19 ms.

TABLE III. Results of the simulated tests.

Test nº	*H*	*T*	H_3	*Err. (H_3)*	T_3	*Err. (T_3)*
1	0.2	2	0.208	0.008	2.012	0.012
2	0.2	3	0,202	0,002	3,008	0,008
3	0.3	2	0,309	0,009	2,041	0,041
4	0.3	3	0.294	-0.006	3.018	0.018
Mean	-	-	-	0.002	-	0.013
RMSD	-	-	-	0.005	-	0.019

*Heights and their respective errors in meters and Periods and their respective errors in seconds.

Simulation Test 3 has been found as a singular case where f_n matches with the third harmonic of the fundamental wave frequency. To assess the effect of the resonance in H_3 estimation this case has been deeply studied. A wave period sweep has been done on the simulation parameters around 3 seconds, maintaining the wave height at 0.3 meters, the WO model parameters and the sea state model (Airy). OrcaFlex results have provided the following results; sea vertical displacement, sea vertical acceleration, drifter vertical displacement and drifter vertical acceleration. In the displacement cases, just the zero-crossing algorithm has been used to obtain H_3, in the acceleration cases, the whole time integration algorithm was considered.

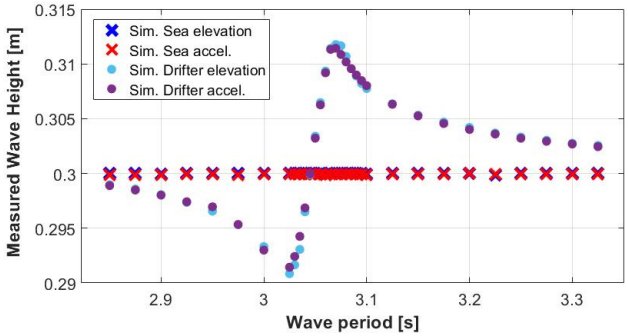

Fig. 5. Effect of the resonance on the obtained significant wave height (H_3) from the OrcaFlex resulting parameters. Blue cross represents the H_3 estimation from the simulated sea elevation, the red cross from the simulated sea acceleration, the blue round from the simulated drifter elevation and the purple round from the drifter acceleration.

Fig. 5 shows the resulting H_3 obtained from the different parameters at the different wave period conditions around 3 seconds. From this figure the algorithm can be validated because with the sea acceleration and displacements the obtained error is below 0.03%. Also, the filtering and integration process does not include significant error because drifter acceleration results are closer to the drifter displacement ones. The major errors are induced when the drifter does not follow the slope of the sea-surface due to the resonance interference. Thus, the maximum error is found when the wave period is 3.06 s, whose third harmonic matches with f_n = 0.98 Hz. In this case, resonance in the vertical acceleration can introduce up to ±1 cm in the wave crests (4% error) because the WO is not strictly following its slope.

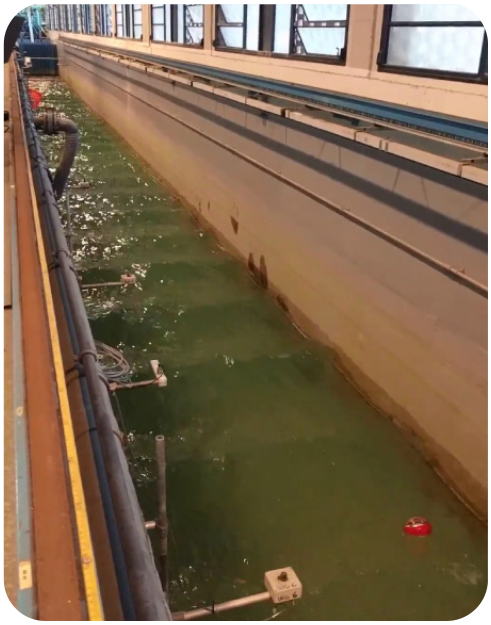

Fig. 6. Channel of Investigation and Marine Experimentation (CIEM) during one of the tests with the drifter.

B. *Experimental results*

This section shows the experimental results of comparing the WL and WO wave parameters estimation among the different tests performed on the CIEM wave plume (Fig. 6). This analysis is summarized on Fig. 7. For this section plots, blue cross represents the channel sensor data, the orange round represents the WL data, the green round represents the WO with KEH data and the purple round represents the WO without KEH data. The channel sensor data has been used as a reference to estimate the errors.

Fig. 7 A. shows the scatterplot with the wave height (y-axis) and wave period (x-axis) results. The distribution of the data shows the different wave parameters set-up of each test (TABLE II), being the test 3 and 4 repeated without the KEH. It can be appreciated that there is a clear bias on both wave parameters since drifters provide lower H_3 and higher T_3. Also, the results dispersion increases with the wave period. Furthermore, the WL data standard deviation has been calculated for each wave condition and it is represented with dashed green lines. Notice that it is centered in the mean values of each test condition. So, for each rectangle, its horizontal width represents the WL wave period standard deviation and the vertical width the WL wave height standard deviation. In some cases, the WO results are not within the dashed rectangle but as it happens both with the KEH (green rounds) and without the KEH (purple rounds), it is not an effect of the KEH.

The distribution of the wave height and period error can be seen on Fig. 7 B. In this plot, x-axis is used for period error and y-axis is used for height error. It can be appreciated that the WO results are closer to the channel sensor results than the WL ones. This may be caused by the higher sampling rates used to acquire the IMU data from WO (SR_{WO} = 50 SPS) compared to the sampling rates used to acquire the IMU data from WL (SR_{WL} = 4-6 SPS). Also, the sampling rate of the channel sensor (SR_{CS} = 40 SPS), used as reference, is closer to the one used on the WO. TABLE IV shows how the WO wave parameters have lower errors than the WL ones. Moreover, results from the WO with the KEH are even lower than the ones without the KEH. On Fig. 7 B it can also be appreciated a dashed blue rectangle corresponding to the root-mean-square deviation (RMSD) of the error, being its horizontal width the RMSD of the period error and its vertical width the RMSD of the height error. This time, it is centered in the mean values of all the WL errors.

TABLE IV. Error results of the experimental tests.

Data	Mean H_3 Err.		Mean T_3 Err.	
	(cm)	(%)	(s)	(%)
WL	-1.85	6.87	0.077	3.12
WO without KEH	-1.81	5.88	0.026	1.16
WO with KEH	-0.72	2.56	0.017	0.82

Fig. 7 C shows the boxplot of the WL wave height results on test conditions 3 and 4. Clearly, there is negative bias on the wave height estimation, but it is also present on the WO results. As already commented, WO results with the KEH are closer to the channel sensor reference and WO results without the KEH are within the WL deviation.

Finally, on Fig. 7 D the spectral analysis of the vertical acceleration (a_z) of the WO is present. Three signals have been compared; the simulated a_z without KEH (yellow), the experimental a_z with KEH (green) and the experimental a_z without (KEH). It is visible that moving mass of the KEH accentuates the PSD on the 1 Hz component of the spectral signal, that corresponds to f_n of the WO and to the third harmonic of the waves ($3 \cdot f_0$). As seen on the Section IIIIII.A,

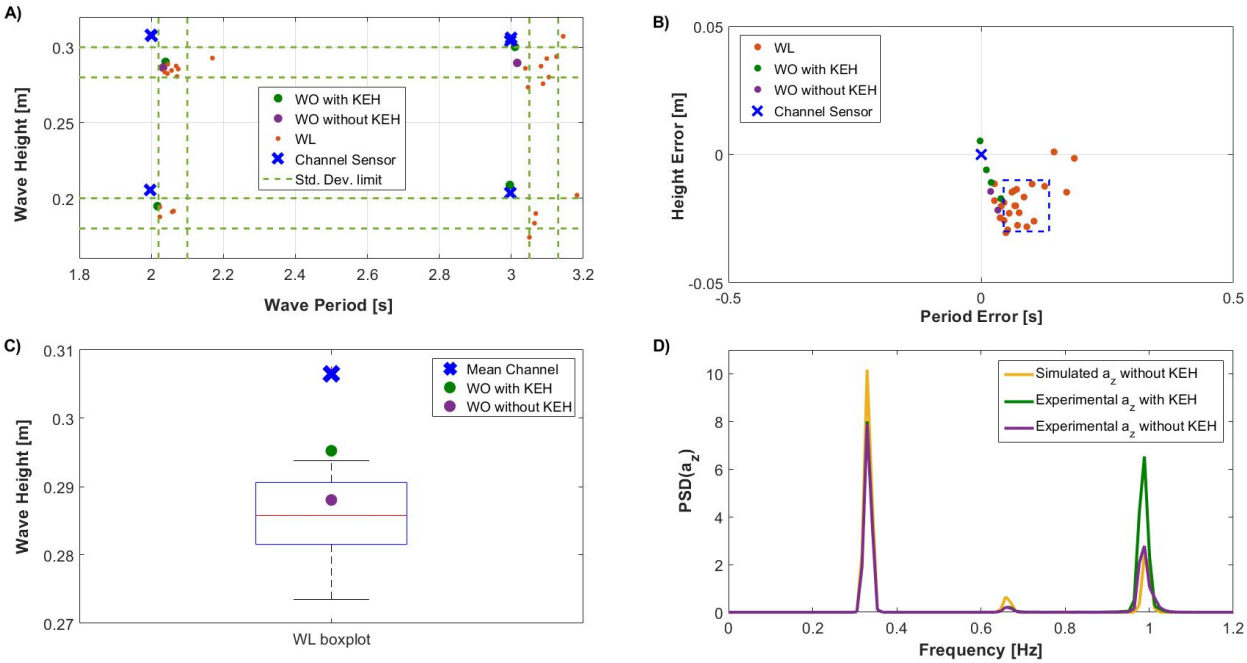

Fig. 7. Experimental analysis results. For all plots, blue cross represents the channel sensor data, the orange round represents the WL data, the green round represents the WO with KEH data and the purple round represents the WO without KEH data. A. Scatterplot with the wave height and period results of the 4 different tests. Green dashed line represents the WL Std. Dev. Limits for each parameter. B. Scatterplot showing the period error at x axis and the height error at y axis, taking the channel sensor data as reference. The dashed rectangle represents the RMSD of the error for each parameter. C. WL data boxplot compared with the WO and the Mean channel sensor data. For this plot, only tests 3 and 4 and their corresponding repetitions have been used. D. Vertical acceleration PSD comparison between simulated a_z without KEH (yellow), experimental a_z with KEH (green) and experimental a_z without (KEH) at test nº 3. In this plot, green line is below purple one.

the algorithm filters these high frequency components to reconstruct D_z, so it should not have a major impact on the wave parameter estimation.

To sum up, it has been found that the WO with KEH results are slightly different from the ones without KEH. In general, all drifters' results show a trend with lower H_3 and higher T_3 than the channel reference. In the case of the significant wave height, it may be because all test conditions are near the resonance wave period excitation, which according to Fig. 5 may cause a reduction on H_3 estimation. Nevertheless, WL results show a similar trend while its f_n is quite different from the WO one (constructive differences). As the wave estimation algorithm has been validated with the simulated data, this general trend may come from the channel uncertainty or from the IMU measurement itself. Despite this, the error induced by the KEH on the H_3 results are within the assumable error that may cause some singular event as resonance. In the case of significant wave periods, mean errors are lower and the effect of introducing a KEH is negligible. Here, differences between WL and WO may come from the differences in the sampling rate between units.

V. Conclusions

The effect of a KEH on the wave parameters estimation at an ocean drifter has been studied. An algorithm has been developed to obtain the sea displacement from the vertical acceleration provided by the embedded drifter's IMU. Then, the zero-crossing method has been used to obtain the significant wave height and period. Simulations performed by OrcaFlex with the Airy wave model have been used to refine the algorithm and estimate its error in critical situations as resonance drifter events. Further, a WO prototype has been deployed in the controlled environment of CIEM wave flume together with four WL units and different sea conditions have been forced. It is concluded that the WO with KEH results are slightly different from the ones without KEH. Nevertheless, in the case of significant wave height (H_3), results are within the assumable error that may cause some singular event as resonance. In the case of significant wave period (T_3), mean errors are lower and the KEH effect is negligible. So, given the current distribution of masses in the WO prototype there is no significant impact on the estimation of the significant wave height and period.

Acknowledgment

The authors extend their thanks to researchers from LIM – UPC for their kind support and yield the facilities of CIEM where the experimental tests were done.

References

[1] "MELOA project." [Online]. Available: https://www.ec-meloa.eu/. [Accessed: 21-Oct-2019].

[2] R. Scharroo *et al.*, "Jason continuity of services: continuing the Jason altimeter data records as Copernicus Sentinel-6," *Ocean Sci.*, vol. 12, no. 2, pp. 471–479, 2016.

[3] T. H. C. Herbers, P. F. Jessen, T. T. Janssen, D. B. Colbert, and J. H. MacMahan, "Observing ocean surface waves with GPS-tracked buoys," *J. Atmos. Ocean. Technol.*, vol. 29, no. 7, pp. 944–959, 2012.

[4] M. Li, S. Zhang, Z. Qi, and C. Dang, "Application of wave drifter to marine environment observation," in *OCEANS 2016 - Shanghai*, 2016, no. 1, p. 5.

[5] P. V. Guimarães *et al.*, "A surface kinematics buoy (SKIB) for wave-current interaction studies," *Ocean Sci.*, vol. 14, no. 6, pp. 1449–1460, 2018.

[6] R. Lumpkin, T. Özgökmen, and L. Centurioni, "Advances in the Application of Surface Drifters," *Ann. Rev. Mar. Sci.*, vol. 9, no. 1, pp. 59–81, 2017.

[7] P. M. Poulain, R. Gerin, E. Mauri, and R. Pennel, "Wind effects on drogued and undrogued drifters in the eastern Mediterranean," *J. Atmos. Ocean. Technol.*, vol. 26, no. 6, pp. 1144–1156, 2009.

[8] M. J. Tucker, "Interpreting directional data from large pitch-roll-heave buoys," *Ocean Eng.*, vol. 16, no. 2, pp. 173–192, 1989.

[9] H. Lin and S. C. S. Yim, "Experimental investigation of stability and bifurcation of nonlinear moored structural responses," in *Proceedings of the International Offshore and Polar Engineering Conference - Montreal*, 1998, vol. 8th, pp. 485–489.

[10] M. Nazari, H. Ghassemi, M. Ghiasi, and M. Sayehbani, "Design of the Point Absorber Wave Energy Converter for Assaluyeh Port," *Iran. J. Energy Environ.*, vol. 4, no. 2, pp. 130–135, 2013.

[11] M. Carandell, D. M. Toma, M. Carbonell, J. del Río, and M. Gasulla, "Design and Testing of a Kinetic Energy Harvester Embedded into an Oceanic Drifter," *IEEE Sens. J.*, no. Advanced Interface Circuits for Autonomous Smart Sensors. Accepted, 2020.

[12] E. D. Skinner, M. M. Rooney, and M. K. Hinders, "Low-cost wave characterization modules for oil spill response," *J. Ocean Eng. Sci.*, vol. 3, pp. 96–108, 2018.

[13] C. E. Duchon, "Lanczos Filtering in One and Two Dimensions," *Journal of applied meteorology*, vol. 18, no. 8. pp. 1016–1022, 1979.

[14] Z. Ballard and B. P. Mann, "Two-Dimensional Nonlinear Analysis of an Untethered Spherical Buoy Due to Wave Loading," *J. Comput. Nonlinear Dyn.*, vol. 8, no. 4, p. 12, 2013.

[15] C. L. Mader, *Numerical Modeling of Water Waves*, vol. 2nd editio. 2004.